Reproducibility of the coil positioning in Nb_3Sn magnet models through magnetic measurements*

F. Borgnolutti, S. Caspi, P. Ferracin, V. V. Kashikhin, G. Sabbi, G. Velev, E. Todesco, A. V. Zlobin

***Abstract*— The random part of the integral field harmonics in a series of superconducting magnets has been used in the past to identify the reproducibility of the coil positioning. Using a magnetic model and a MonteCarlo approach, coil blocks are randomly moved and the amplitude that best fits the magnetic measurements is interpreted as the reproducibility of the coil position. Previous values for r.m.s. coil displacements for Nb-Ti magnets range from 0.05 to 0.01 mm. In this paper, we use this approach to estimate the reproducibility in the coil position for Nb_3Sn short models that have been built in the framework of the FNAL core program (HFDA dipoles) and of the LARP program (TQ quadrupoles). Our analysis shows that the Nb_3Sn models manufactured in the past years correspond to r.m.s. coil displacements of at least 5 times what is found for the series production of a mature Nb-Ti technology. On the other hand, the variability of the field harmonics along the magnet axis shows that Nb_3Sn magnets have already reached values similar to thise obtained for Nb-Ti ones.**

***Index Terms*—Field quality, superconducting accelerator magnets.**

I. INTRODUCTION

THE shape of the field lines in a superconducting magnet is mainly given by the ability to precisely position the coil blocks around the beam tube [1-3]. The main difficulty stems from the fact that a shift of the conductor position of a fraction of a millimeter in the transverse plane can produce relative field errors of the order of 0.1%. On the other hand, the precision required from the beam dynamics constraints is one order of magnitude better [3]. This field homogeneity has to be reached over a significant fraction of the magnet transverse aperture (usually 2/3), where the beam is located. Simulations show that the precision in the position of the coil blocks to reach this field homogeneity has to be of the order of 0.01 to 0.05 mm [4-7]. This is particularly challenging since magnets are assembled with a coil prestress of the order of 20 to 150 MPa to be able to avoid movements due to the large electromagnetic forces arising during powering. This precision also sets the tolerances for the magnet components around the coil.

A systematic offset in the position of the coil is easy to cure through a fine tuning of the cross-section. For this reason one usually leaves some free parameters in the design such as shims that can be used to trim field quality. On the other hand, very little can be done for the random variations of the position of the coil, which is mainly due to the reproducibility of the industrial process of the coil manufacturing and assembly [4-8]. In principle, some limited feed-back could be done during production after room temperature magnetic measurements to cancel the largest harmonics, but this has a large impact on the costs and delays the production. Some optimization can be done during magnet installation by appropriate placing of magnets based on their field quality. In most cases, one has to live with this random part, which sets the ultimate limit to have a pure multipolar field.

Given a set of magnets, the spread in the measured multipoles can be interpreted as a spread in the position of the coil using a MonteCarlo simulation [7,8]. The measurements of Nb-Ti magnets during the past 30 years have shown that this spread ranges from 0.06 to 0.01 mm (one sigma). These data refer to a stable production of the same object, with the number of pieces ranging from 10 to 1000.

Nb_3Sn coils have a different manufacturing process different from Nb-Ti coils. In the latter case the precise coil geometry in a magnet can be provided by the precise mechanical structure (collar). Thus, the large tolerances in the coil size do not cause a large spread in the coil positioning. For instance, in the LHC dipoles the azimuthal coil size has been controlled within ±0.15 mm, nevertheless, the spread in the coil position evaluated from the magnetic measurements is at least a factor of 3 lower. On the other hand, the state-of-the-art Nb_3Sn coil technology, its high coil rigidity and the superconductor brittleness limit the possibilities of coil geometry control by the shape of the retaining structure.

For Nb_3Sn magnets, aiming at reaching ~50% larger peak fields in the coil than Nb-Ti, most of the attention has been devoted up to now to the magnet quench performance. Today, thanks to the high-field magnet program at Fermi National Laboratory (FNAL) core program [9-11] and to the US-LHC Accelerator Research Program (LARP) Technological Quadrupole (TQ) [12,13], we have a small series of nearly identical Nb_3Sn dipole and quadrupole models which allow assessing the precision of the reproducibility in coil positioning for this new technology.

Manuscript received August X, 2008.

F. Borgnolutti and E. Todesco are with CERN – Accelerator Technology department, Geneva 23, 1211 CH (phone: +41-22-767-3291; fax: +41-22-767-6300; e-mail: ezio.todesco@cern.ch).

S. Caspi, P. Ferracin, G. Sabbi are with Lawrence Berkeley National Laboratories.

V. V. Kashikhin, G. Velev, A. V. Zlobin are with Fermi National Accelerator Laboratory.

*This work was supported by the U.S. Department of Energy under Contract No. DE-AC02-05CH11231.

In Section II we briefly outline the method used to estimate the reproducibility of the coil positioning from the spread of the field harmonics. Moreover, we recall the results which have been obtained for the Nb-Ti magnets, which are used as a benchmark. In Section III we apply the method to analyze the data of the six FNAL High Field Dipole (HFD) magnets, and to the six Technological Quadrupole (TQ) models built by the US LARP collaboration between Lawrence Berkeley National Laboratories, Brookhaven National Laboratory, and FNAL. Conclusions are drawn in Section IV.

II. A Monte-Carlo approach to estimate the reproducibility of coil positioning through magnetic measurements

A. A review of the method

A standard way of estimating the random component of the field quality in a superconducting magnet is based on a MonteCarlo simulation [4-8]. Each coil block is moved independently along the three degrees of freedom, i.e. radial movement, azimuthal movement, and tilt (see Fig. 1). Three independent random numbers are drawn for each coil block, with the same amplitude. To be more precise, let (r,θ) be the coordinates of the block baricentre, and ρ the distance of the block corner from the baricentre. The block will be moved by

$$\begin{aligned} \Delta r &= \frac{d}{\sqrt{3}}\varepsilon_1 \\ \Delta\varphi &= \frac{d}{r\sqrt{3}}\varepsilon_2 \\ \Delta\alpha &= \frac{d}{\rho\sqrt{3}}\varepsilon_3 \end{aligned} \tag{1}$$

where ε_1, ε_2 and ε_3 are three independent dimensionless random variables with zero average and sigma equal to one, and d is the rms value of the displacement. We used Gaussian random variables to simulate components and assembly tolerances; in principle, a uniform distribution can also be considered.

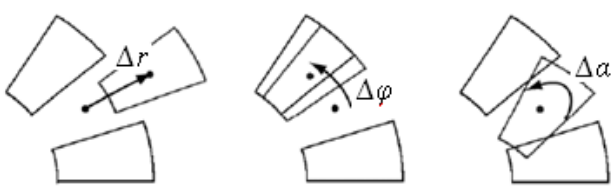

Fig. 1. Displacements associated with the position of a block in the coil transverse cross-section.

Once such random movements are assigned to the cross-section, the magnetic field is computed for this new configuration which is supposed to simulate a real coil including the manufacturing and assembling imperfections. The field is then represented according to the standard multipolar expansion

$$B(z) = 10^{-4} B_N \sum_{n=1}^{\infty} (b_n + i a_n) \left(\frac{z}{R_{ref}} \right)^{n-1} \tag{2}$$

where R_{ref} is a reference radius used to have dimensionless multipoles, and B_N is the main harmonic, i.e. N=1 for a dipole and N=2 for a quadrupole, and by definition $b_N=10^4$. The simulation is repeated for 100-1000 cases, and an average $\mu_n(d)$ and standard deviation $\sigma_n(d)$ of the field harmonics is estimated for a given amplitude d. The standard deviation $\sigma_n(d)$ represents the impact of the spread d of the coil position on the field harmonics.

One finds that the spread in the multipoles is proportional to the spread in the position d within the interesting domain (d=0.01 to 0.2 mm). Moreover, one finds that normal and skew components of the same order have a similar spread (within a few percent), the normal-skew symmetry being slightly broken by the tilt movement [8]. Finally, the spread in the multipoles roughly decays with the multipole order n as $(R_{ref}/r)^n$, where r is the aperture radius, as expected by the Biot-Savart law. The error associated to the estimate of d is of the order of 20% to 60% [7].

Summarizing, in a semi-logarithmic plot $\log(\sigma_n)$ versus multipole order n as shown in Fig. 2 the Monte-Carlo results will be close to straight lines. By comparing with the results of magnetic measurements, one can finally evaluate the best value of d that accounts for the measured spread. The fit has to be done in the semilogarithmic scale otherwise the higher order contribution is negligible [7,8]. The comparison of the data with simulation usually points out a knee in the measurement data, which is due to the finite resolution of the measurement. For this reason, one has to perform the fit using data up to a given multipolar order, which is usually ranging between 8 and 12. In Fig. 2 we show the case of the LHC interaction region quadrupole MQXA, where the noise of the measurement is about 0.007 units and the truncation order for the fit has been set to 8.

The second important feature of the fit is that allow multipoles always have a larger spread than the non allowed ones of the same order. A more detailed modeling consists of having a separate fit, and therefore different estimates of the spread d, for each family of multipoles [4,7,8]. This method will be used for the dipoles in Section III.A.

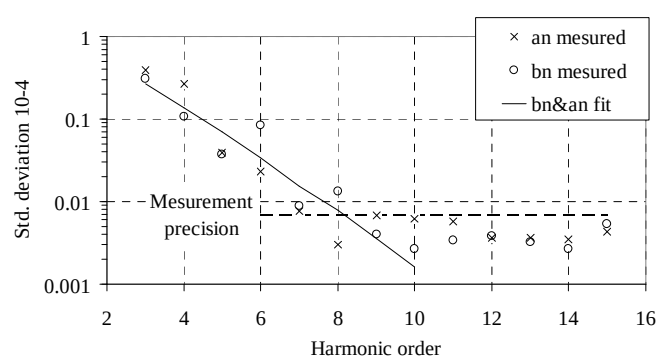

Fig. 2. Standard deviation of the multipoles measured in the LHC MQXA quadrupoles (markers), and best fit simulated for a random displacement of the coils of 0.011 mm (lines). The measurement precision is shown to be about 0.007 units (dashed line).

The spread of the integral harmonics measured over the

production of Tevatron, HERA, RHIC and LHC is given in Table I [8]. R. m. s. coil displacements range from 0.065 mm in Tevatron to 0.016 mm in RHIC, i.e. a gain of factor four has been reached by this technology over 30 years. The level of complexity of the coil design is also important: the double layer, six block, 30 mm width coil in the LHC dipoles has a larger spread than the single layer, four blocks, 10 mm width coil in the RHIC dipoles.

TABLE I
Estimate of the reproducibility of the coil positioning in the production of superconducting dipoles (in mm) for 4 high energy particle accelerators, average values and split among the different multipole families [7].

Magnet	b_{2n+1}	b_{2n}	a_{2n+1}	a_{2n}	all
Tevatron	0.128	0.052	0.070	0.052	0.065
HERA	0.122	0.020	0.024	0.058	0.041
RHIC	0.052	0.006	0.008	0.032	0.016
LHC	0.054	0.001	0.018	0.026	0.025

It is well known that the random movements are not equally spread along the different degrees of freedom: one systematically observes that the spread in odd normal multipoles is 2-3 times larger than in the skew, and vice versa for the even ones [4-8]. For this reason we also report the decomposition of the spread for each multipole family: in RHIC and LHC, the odd normal multipoles (i.e., the "allowed ones") correspond to a spread of around 0.050 mm, whereas the other ones range between 0.005 to 0.030 mm.

Indeed, there are additional features to be taken into account. The spread of the integral harmonics over a set of homogeneous magnets built on the same design, and the corresponding spread in the coil position as given in Table I, depends on two components. The first one is the spread along the magnet axis, integrated over the total magnet length. This spread *depends on the magnet length*, and becomes negligible for very long magnets as the LHC dipoles.

The second component is due to the coil itself: this does not vary along the coil length, but it rather depends on assembly features that are common to the coil as a whole and differ from coil to coil (as for instance the curing cycle or the collaring). This second component *does not depend on the magnet length*.

The spread of the integral harmonics over a set of magnets will be the sum of the spread along the axis, plus the spread from coil to coil. For the long magnets given in Table I, the second component is overwhelming. For example, in the LHC 14.3-m-long dipoles the spread along the axis measured with 125-mm-long mole correspond to about 0.030 mm of spread in the coil position. In the hypothesis of a Gaussian distribution of the spreads along the axis, this gives a negligible contribution (about 0.003 mm) to the spread along 14.3 m. For a 1-m-long model of the LHC dipole, the contribution of the spread along the axis would be 0.012 mm, i.e. still small but not negligible w.r.t. 0.025 mm spread from coil to coil.

In conclusion, some care shold be taken when carrying out this analysis to be sure that the spread along the axis and the magnet length are taken into account, and that the correct physical interpretation is given to these quantities computed from measurements and simulations.

For the Nb-Ti quadrupoles in RHIC and LHC, results are summarized in Table II. The spread ranges from 0.01 mm to 0.03 mm. Also in this case one can conclude that the spread along the axis is negligible w.r.t. the spread from coil to coil.

TABLE II
Estimate of the reproducibility of the coil positioning in the production of superconducting quadrupoles for RHIC and LHC.

Magnet	d (mm)
RHIC MQ	0.022
RHIC MQY	0.018
LHC MQ	0.029
LHC MQY	0.025
LHC MQXA	0.010
LHC MQXB	0.016

III. Analysis of the Nb_3Sn models

A. *FNAL HFDA dipoles*

The HFDA dipole has been designed as a part of the FNAL high field magnet program in support of the R&D effort for the Very Large Hadron Collider (VLHC). It is based on the Nb_3Sn technology using the react-and-wind method and aims at producing a bore field above 10 T [9-11]. The design is based on a two layers coil with a 43.5 mm diameter bore (see Fig. 3) surrounded by a cold iron yoke. The cable width is ~15 mm, thus giving a coil width of ~30 mm. Six nearly identical 1-m-long dipole models, named HFDA02 to HFDA07, have been built and tested. The magnets have the same cross-section and same cable geometry.

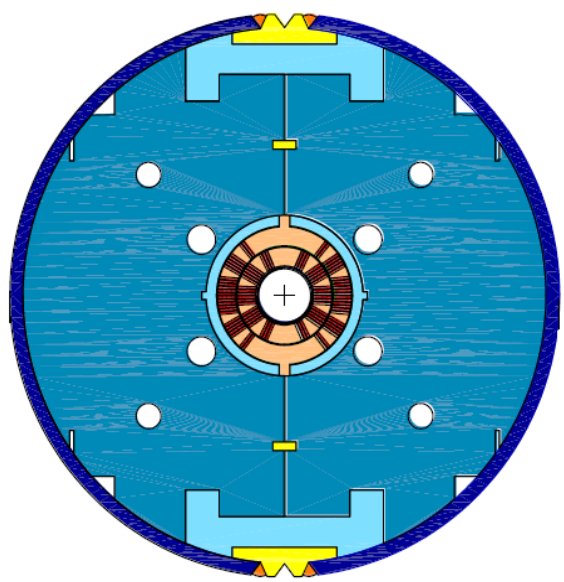

Fig. 3. Cross-section of the HFDA dipole coil [11].

The six models use different mid-plane and radial shims to optimize the coil pre-stress (i.e. to compensate for different coil sizes), which is a very sensitive quantity for the Nb_3Sn.

This obviously increases the spread in the field harmonics. This effect is subtracted by using the sensitivity tables of multipoles versus shim size evaluated through a electromagnetic model. The strand for the first three models HFDA02-04 was produced using the Modify Jelly Roll (MJR) process, while the three last models HFDA05-07 use Powder-in Tube (PIT) made strand. The diameter of both strands and the cable geometry are the same and therefore it should not affect the field quality. The geometric harmonics of the six magnets, presented in Table III for a reference radius of 10 mm, are obtained averaging the multipole values between the current up and down ramps at 3 kA to subtract the coil magnetization and the iron yoke hysteresis effects. The magnets were pre-cycled up to a high current prior to each measurement to remove the possible magnetization history effect.

Using the Montecarlo method described in the previous section, we obtain an estimate of the spread in the position of the coil of 0.13 mm (see Fig. 4). This number is about 2 times larger than that obtained for the Tevatron dipoles, and 5 times the LHC dipoles. Here, we have to point out that we are comparing a stable series production of a well–established technology with a new technology used in a few models. The data split according to the different families are shown in Table IV. Unfortunately, no measurement of the spread along the axis is available and therefore we cannot separate in this 0.13 mm estimate the part coming from the spread from coil to coil from the part coming from the variation along the axis.

TABLE III
Integral harmonics of the 6 model HFDA02-07, average between up and down ramp at 3 kA, and standard deviation.

HFDA	02	03	04	05	06	07	Std. dev.
b2	4.1	-7.13	0.75	4.59	-3.63	0.42	4.53
b3	-4.0	-2.36	8.28	1.16	3.78	5.52	4.71
b4	0.4	-0.19	0.16	0.79	-1.52	-0.02	0.79
b5	0.0	-0.53	-0.34	1.94	1.20	1.35	1.02
b6	0.0	0.12	0.02	0.22	-0.30	-0.06	0.18
b7	0.1	0.04	0.49	0.29	0.17	0.09	0.17
b9	-0.2	-0.01	-0.15	0.1	0.07	-0.08	0.12
a2	-9.6	1.93	12.56	-0.45	-8.22	1.57	8.04
a3	-0.2	0.81	-0.25	0.90	1.10	0.91	0.60
a4	-1.1	-0.75	0.06	-1.97	-1.31	0.67	0.96
a5	0.3	0.04	0.11	0.26	0.25	0.06	0.11
a6	0.3	0.03	-0.01	-0.28	-0.39	0.09	0.25
a7	-0.1	0.03	-0.03	0.03	0.08	0.03	0.06
a9	-0.2	0.04	-0.07	-0.01	-0.10	0.21	0.14

TABLE IV
Estimate of the reproducibility of the coil positioning (in mm) in the production of superconducting dipoles for HFDA, average values and split among the different multipole families.

Magnet	b_{2n+1}	b_{2n}	a_{2n+1}	a_{2n}	all
HFDA	0.274	0.124	0.047	0.180	0.130

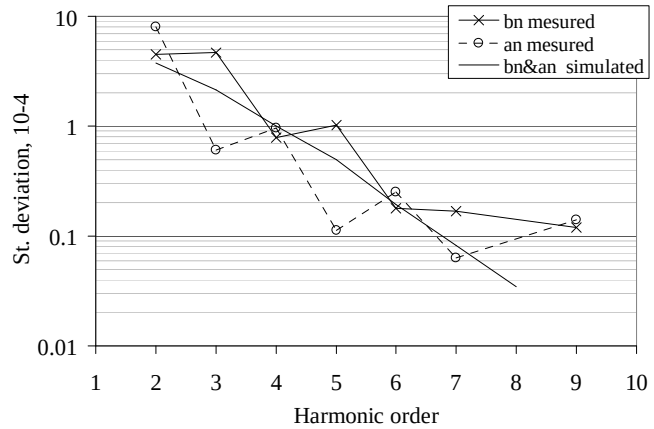

Fig. 4. Standard deviation of the multipoles of the 6 HFDA Nb_3Sn dipole magnets (markers), and estimate of the standard deviation for a random movement of the blocks of 0.13 mm (solid line) (R_{ref}=10 mm).

An indirect cross-check of this result comes from the measurement of the coils position in the HFDA02 cross-section carried out at Fermilab on a slice of the magnet using an optical system [11]. For each block one has four measurements (one per quadrant), and average and standard deviations are computed. The standard deviations are given in Table V. The block numbering starts from the inner layer mid-plane block, and ends at the outer layer pole block. The average random displacement for each degree of freedom ranges from 0.05 mm for the tilt, to 0.12 for the azimuthal movement. Summing the three values in quadrature one obtains 0.15 mm.

TABLE V
Estimate of the reproducibility of the coil positioning in the production of superconducting dipoles for HFDA, average values and split among the different multipole families.

Block	Δr (mm)	$\Delta\phi$ (mm)	$\Delta\alpha$ (mm)
1	0.110	0.173	0.061
2	0.115	0.120	0.050
3	0.076	0.090	0.035
4	0.090	0.122	0.089
5	0.062	0.129	0.047
6	0.012	0.092	0.028
average	0.078	0.121	0.052

B. LARP TQ quadrupoles

The 90 mm aperture Technological Quadrupoles (TQ) [12,13] have been designed in the frame-work of the LARP program aiming at demonstrating viability of Nb_3Sn quadrupole magnets for the upgrade of the LHC interaction regions. The TQ coil cross-section is made of two layers wound with a 10 mm width cable.

Two different coil support structures have been studied for the same coil cross-section: the TQS and TQC types (see Figs. 5 and 6). The TQC coil is pre-stressed and supported by round stainless steel collars, 2-piece iron yoke and stainless steel skin [12] while the TQS coil is pre-stressed by thick aluminum cylinder through 4-piece iron yoke [13]. Since the TQ

program has been launched, six TQS (TQS01a/b/c and TQS02a/b/c) and five TQC (TQC01a/b and TQC02a/b/e) quadrupole magnets have been built and tested. The versioning of the magnets (a-b-c) is related to a reassembly of the magnet and replacement of faulty coils. TQC02e denotes a quadrupole based on the collar structure that used coils which were already tested in TQS02. Since we are interested in the spread of the coil positioning caused by assembly and components, we carried out a simulation on the spread evaluated on the available data, namely four TQS and three TQC.

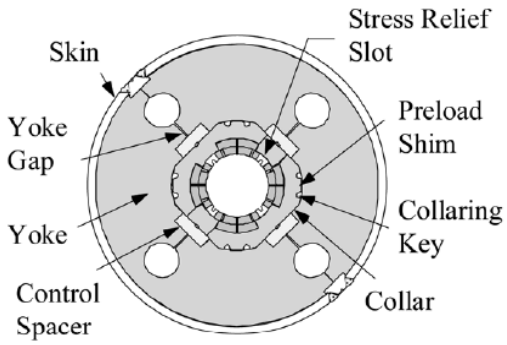

Fig. 5. Cross-section of the 90mm aperture TQC type quadrupole magnet [10].

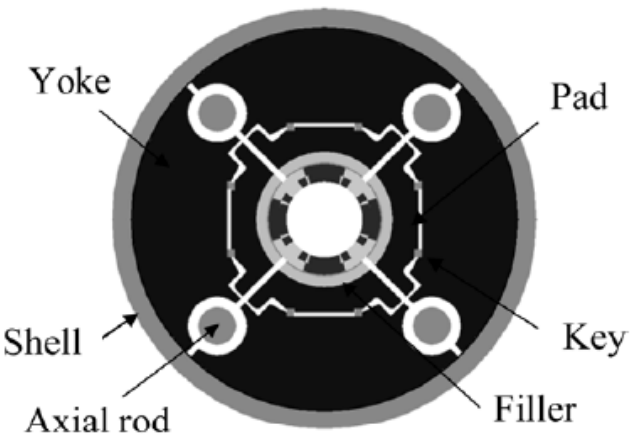

Fig. 6. Cross-section of the 90mm aperture TQS type quadrupole magnet [10].

TQS and TQC have a different design and cross-section of the yoke but the same coil, which cause a difference in b_6 and b_{10}. This difference is subtracted to have a homogeneous set of data. The available data and the spread are given in Table VI. The best fit of the MonteCarlo is shown in Fig. 7. The corresponding spread in the coil positioning is 0.144 mm. Also in this case, this is at least a factor 5 worse than what is obtained for a mature production of Nb-Ti quadrupoles.

TABLE VI
TQ integral harmonics at 45 T/m, R_{ref} = 22.5 mm. Calculated values of b_6 and b_{10} *are* subtracted.

	TQC			TQS				
n	01a	02e	02a	01a	02a	02b	02c	St. dev.
b3	0.99	-0.01	-3.40	-1.49	1.90	0.60	-2.62	1.97
b4	-0.07	0.41	2.07	-1.13	1.28	2.38	3.26	1.53
b5	2.89	4.65	-5.33	-0.83	2.66	-0.46	-1.11	3.33
b6	-6.28	-7.12	-7.03	-6.33	-6.75	-7.25	-7.88	0.56
b7	0.13	-0.10	-0.11	0.19	0.00	0.11	-0.19	0.14
b8	-0.06	0.08	0.20	-0.05	-0.29	0.02	0.01	0.15
b9	-0.04	-0.07	0.21	0.12	0.15	-0.04	0.04	0.11
b10	0.02	0.24	0.12	0.22	0.10	0.33	0.30	0.11
a3	-1.54	0.43	-2.95	3.64	2.55	-7.02	-6.62	4.19
a4	-0.63	-2.33	4.38	-3.34	-5.87	0.73	0.85	3.33
a5	5.00	8.35	6.83	-0.78	-0.38	1.17	-1.33	3.97
a6	0.03	0.52	-1.58	-0.26	-0.08	-0.61	0.79	0.78
a7	0.07	-0.50	-0.22	-0.29	-0.15	0.06	-0.02	0.21
a8	0.12	0.26	-0.48	-0.16	-0.56	0.13	-0.08	0.31
a9	-0.04	-0.24	-0.33	-0.01	-0.05	0.04	0.00	0.14
a10	-0.01	0.04	0.03	0.02	-0.09	0.00	0.02	0.04

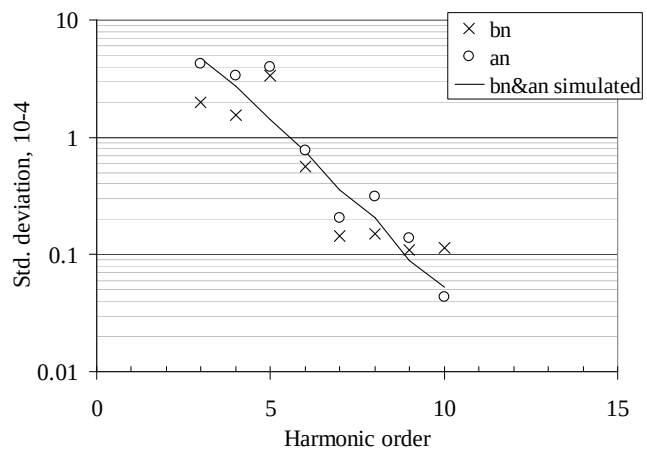

Fig. 7. Standard deviation of six TQ magnets (markers), and best fit through simulation (lines) with d = 0.144 mm.

A few TQ models (TQS01a, TQS02a, TQC02a and TQC02e) have also been measured with 100 mm long rotating coils; in this case we have 5 measurements in consecutive positions that are in the so-called straight part of the magnet. A spread computed over five measurements can provide a rough estimate of the precision of the coil positioning along the magnet axis. Results are shown for TQC02e in Fig.8: the fit gives a spread in the coil position of 0.036 mm. For other three magnets one finds similar values, see Table VII. One can draw the following conclusions:

- The spread along the axis measured with a 100-mm long-mole in Nb3Sn quads is similar to what is measured in the main LHC dipoles with a 125-mm long-mole.
- The reproducibility of the position of 0.14 mm estimated through the spread of the integrals is dominated by the spread from coil to coil, and not from the spread along the axis. The contribution along the axis, integrated over the 0.8 straight part

of the magnet, gives about 0.015 mm, i.e. one order of magnitude less.

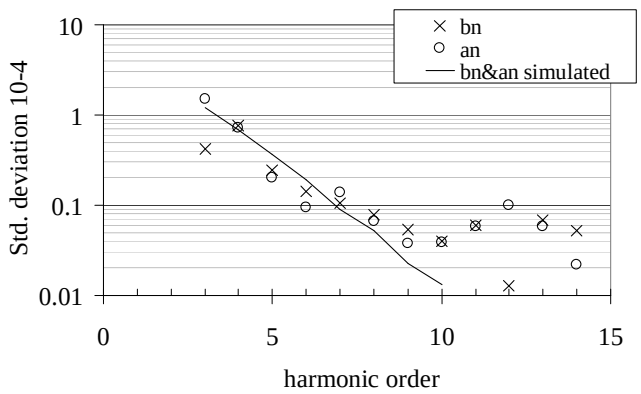

Fig. 8. Standard deviation of multipoles (markers) along the axis of TQC02e, (measurements with a 0.1 m long coil at 22.5 mm reference radius), and Monte Carlo best fit with 0.036 mm spread in the coil position (lines).

TABLE VII
Estimate of the reproducibility of the coil positioning along the axis for three TQ quadrupoles.

Magnet	d (mm)
TQS01a	0.042
TQS02a	0.045
TQC02a	0.064
TQC02e	0.036
LHC dipoles	0.030

IV. Conclusions

In this paper we studied the reproducibility that can be obtained in positioning the coil in superconducting magnets made with Nb_3Sn coils, and we compared it to the results relative to the standard technology based on Nb-Ti. This reproducibility usually sets the ultimate limit to the field quality that can be achieved in superconducting magnets for high energy particle accelerators.

The computations are based on an inverse method that makes use of a MonteCarlo analysis: the relation between the spread in the coil position and the spread in the field harmonics is evaluated with a standard code that implements the Biot-Savart law. Then, the spread in the integral field harmonics measured over a homogeneous series of magnets is associated with a spread in the coil position through a best fit.

Some care must be taken to separate the component coming from the variation along the magnet axis, which depends on the magnet length, from the part that varies from coil to coil.

Reference values set by the Nb-Ti technology used in high energy particle accelerators have been reviewed. For both dipoles and quadrupoles manufactured in the past 15 years the measured spread in field harmonics corresponds to a coil position reproducibility (from magnet to magnet) of 0.030 to 0.015 mm, reaching a minimum of 0.010 for the LHC MQXA. These values are obtained for a mature technology and for a stable production of several units (20 to 1000) of the same objects. Oldest magnets, namely Tevatron and HERA dipoles, have a larger spread of 0.040 to 0.065 mm. Measurements with a short mole on the LHC dipoles indicate that the contribution coming from the spread along the axis is negligible for these long magnets, and that these values do not depend on the magnet length.

For the Nb_3Sn accelerator magnet technology the analysis was performed for two small series of 1-m-long R&D models which include 6 43.5-mm HFDA dipoles and 6 90-mm TQ quadrupoles. We obtain a spread of 0.13 mm for the dipoles and 0.14 mm for the quadrupoles. In the first case, the estimate based on the magnetic measurements is in good agreement with an optical measurement carried out over a slice of the magnet. Part of the difference between the Nb-Ti and the Nb_3Sn values are due to the fact that we are comparing a few R&D short models with a mass production. Therefore, it is premature to conclude that the Nb_3Sn technology is intrinsically providing a worse field quality than the Nb-Ti. There is still the potential of an improvement of a factor 5-10.

We also analyzed the spread in the coil position along the axis of the same magnet. As for Nb-Ti long dipoles, this quantity does not affect the spread from magnet to magnet and therefore the 0.14 mm previous estimate does not depend on the fact that we are considering very short models. On the other hand, the 0.03 mm spread along the axis obtained with a 100 mm long mole for the TQ is very similar to what is obtained for the LHC dipole with a similar mole length (125 mm). This means that the homogeneity of the field quality along the axis of a Nb_3Sn magnet has nearly reached the standards of the Nb-Ti technology.

References

[1] H. Brechna, “Superconducting magnet systems”, (Springer, Berlin, 1973).
[2] M. N. Wilson, “Superconducting magnets”, (Clarendon Press, Oxford, 1983)
[3] K. Mess, P. Schmuser, S. Wolff, “Superconducting accelerator magnets”, (World Scientific, Singapore, 1996).
[4] J. Herrera, et al., *Particle Accelerator Conference* (1985) 3689.
[5] R. Gupta, *Part. Accel.* **56** (1996) 111.
[6] P. Ferracin, W. Scandale, E. Todesco, R. Wolf., *Phys. Rev. STAB* **3** (2000) 112403.
[7] B. Bellesia, C. Santoni, E. Todesco, *European Particle Accelerator Conference* (2006) 2601, and B. Bellesia, J. P. Koutchouk, E. Todesco, *Phys. Rev. STAB* **10** (2007) 062401.
[8] J. Herrera, et al., *Particle Accelerator Conference* (1987) 1477.
[9] A. V. Zlobin, et al, *Particle Accelerator Conference* (2007) 482.
[10] G. V. Velev, et al., *IEEE Trans. Appl. Supercond.* **18** (2008) 184.
[11] V. V. Kashikhin, et al., *Particle Accelerator Conference* (2005) 366.
[12] S. Feher, et al., *IEEE Trans. Appl. Supercond.* **17** (2007) 1126.
[13] S. Caspi, et al., *IEEE Trans. Appl. Supercond.* **17** (2007) 1122.